Available online at www.sciencedirect.com
ScienceDirect
Nuclear Instruments and Methods in Physics Research B 255 (2007) 124–129
NIM B
Beam Interactions with Materials & Atoms
www.elsevier.com/locate/nimb

# Structure and stability of irradiation-induced Frenkel pairs in 3C-SiC using first principles calculations

G. Lucas *, L. Pizzagalli

*Laboratoire de Métallurgie Physique (UMR6630-CNRS), SP2MI, Bd Marie et Pierre Curie, BP 30179, 86962 Futuroscope-Chasseneuil Cedex, France*

Available online 21 December 2006

**Abstract**

We have performed first principles calculations of intrinsic point defects and Frenkel pairs in cubic silicon carbide, using generalized gradient approximation. The considered Frenkel pairs have been obtained from a previous work on the determination of threshold displacement energies [G. Lucas, L. Pizzagalli, Phys. Rev. B 72 (2005) 161202]. Structures and formation energies of the defects are described. We found that our GGA results are in very good agreement with previous LDA studies. We found that Frenkel pairs are more stable than isolated single defects, especially for silicon interstitials, pointing to an attractive interaction between vacancies and interstitials as expected.


*PACS:* 68.55.Ln; 81.05.Je; 71.15.Mb

*Keywords:* Silicon carbide; First principles calculations; Point defects; Irradiation

## 1. Introduction

Silicon carbide is largely studied due to its possible use in eletronics, as a replacement for silicon in specific applications, or in nuclear environments. In particular, there is a strong interest for understanding the behavior of silicon carbide under irradiation. Several mechanisms such as defects creation from cascades, amorphization, swelling, or crystal recovery are still actively investigated. A fundamental quantity for describing damage creation in a material is the threshold displacement energy. Several theoretical works have been devoted to their determination in silicon carbide [1–6]. Recently, we have performed first principles molecular dynamics calculations for computing the displacement energies in 3C-SiC [7]. Several directions have been considered, each threshold energy being associated with a specific Frenkel pair configuration. Due to the large number of runs and the long time associated with each molecular dynamics run, these simulations have been performed in small cells, encompassing 64 or 96 atoms. These limited sizes lead to a large uncertainty, about 1 eV, on the computed displacement energies. However, regarding the magnitude of the determined values, such an inaccuracy is more than acceptable.

It is important to fully characterize the Frenkel pairs obtained during the determination of displacement energies. In particular, interesting data are the structure and formation energy of the Frenkel pairs. The latter may be compared to single point defects energies, in order to gain information about crystal recovery. The aim of this paper is to describe and discuss the structure and stability of Frenkel pairs, obtained during displacement energy determinations [7], compared to single point defects. In this case, a 1 eV uncertainty is not acceptable and previously determined Frenkel pairs have been relaxed in larger cells. Also, we used generalized gradient approximation (GGA) to investigate the effect of exchange correlation functional on the stability, since available studies in 3C-SiC are usually performed within local density approximation (LDA).

After a brief description of the method, we will first report the structure and the energies of intrinsic point

* Corresponding author. Tel.: +33 5 49 49 68 30; fax: +33 5 49 49 66 92.
*E-mail address:* guillaume.lucas@etu.univ-poitiers.fr (G. Lucas).

0168-583X/$ - see front matter © 2006 Elsevier B.V. All rights reserved.
doi:10.1016/j.nimb.2006.11.047

defects in 3C-SiC. Then, the structure and formation energy of Frenkel pairs will be described. In a third section, we will discuss our results.

## 2. Computational method

Total energy calculations have been performed within the framework of the density functional theory (DFT) [8,9], using the plane-wave pseudopotential Quantum-ESPRESSO package [10]. The Perdew-Burke-Ernzerhof GGA expression is employed for the exchange-correlation functional [11].

Intrinsic defects and Frenkel pairs have been modelled using periodic supercells with 216 crystal lattice sites, in order to limit artificial defect–defect interaction. Due to the large cell size, a $\Gamma$ sampling of the Brillouin zone is enough to provide converged defects energies. Vanderbilt ultra-soft pseudopotentials [12] and a plane-wave basis set are employed for the carbon and the silicon. With these pseudopotentials and a basis set including plane-waves of a kinetic energy up to 25 Ry, defect formation energies have been calculated with a convergence error below 0.1 eV.

For each defect configuration, configurations have been relaxed using a Broyden-Fletcher-Goldfarb-Shanno (BFGS) algorithm [13]. The formations energies of points defects have been calculated following the formalism by Zhang and Northrup [14]. The chemical potential of silicon and carbon calculated in the diamond phase with the theoretical equilibrium lattice constant have been used.

## 3. Intrinsic point defects

Relevant insights about the formation of intrinsic point defects during irradiation processes may be obtained by investigating their stability, what is easily determined by computing formation energies. They obviously depend on the conditions silicon carbide material is found. For instance, p-type materials favor the appearance of positively charged defects, whereas n-type materials favor negatively charged defects. Moreover, a material is not necessarily in stoichiometric conditions and the formations energies of point defects are different in carbon-rich conditions and silicon-rich conditions. Carbon based defects are more stable in silicon-rich conditions and inversely.

Intrinsic point defects typically include vacancies, antisites and interstitials. Presented in Table 1, formation energies of a large set of point defects have been calculated at their neutral charge state in stoichiometric conditions. They are compared with previous calculations, all made using the local density approximation (LDA), with and without spin polarization [15–18].

### 3.1. Vacancies

In silicon carbide, a much harder material than silicon, the mobility of point defects is clearly reduced. Because of the stronger chemical bonding, vacancies are thermally stable at room temperature and above.

Table 1
Calculated formation energy in eV of intrinsic defects in the neutral charge state for the ideal stoichiometry

| Defect | This work | [15] | [16] | [17] | [18] |
|---|---|---|---|---|---|
| *Vacancies* | | | | | |
| $V_C$ | 3.63 | 3.74 | 4.2 | 4.30 | |
| $V_{Si}$ | 7.48 | 8.38 | 8.1 | 8.45 | |
| *Antisites* | | | | | |
| $C_{Si}$ | 3.48 | 3.28 | 3.4 | | |
| $Si_C$ | 4.02 | 4.43 | | | |
| *Carbon interstitials* | | | | | |
| $C_{TC}$ | $CC_{\langle 100\rangle}$ | 10.22 | | | $H_C$ |
| $C_{TSi}$ | $CC^*_{\langle 100\rangle}$ | 9.82 | | | $CSi_{\langle 100\rangle}$ |
| $CC_{\langle 100\rangle}$ | 6.47 | | 6.9 | | $W_C$ |
| $CC^*_{\langle 100\rangle}$ | 6.31 | | | | |
| $CC_{\langle 110\rangle}$ | 6.65 | | | | 6.7 |
| $CSi_{\langle 100\rangle}$ | 6.94 | | | | 6.5 |
| $CSi_{\langle 110\rangle}$ | $CC^*_{\langle 100\rangle}$ | | | | $W_C$ |
| $H_C$ | 8.21 | | | | 7.6 |
| *Silicon interstitials* | | | | | |
| $Si_{TC}$ | 7.04 | 7.02 | | | 6.0 |
| $Si_{TSi}$ | 9.23 | 9.13 | | | 8.4 |
| $SiSi_{\langle 100\rangle}$ | 9.32 | | | | $Si_{TC}$ |
| $SiSi_{\langle 110\rangle}$ | 8.11 | | | | 7.4 |
| $SiC_{\langle 100\rangle}$ | $SiSi_{\langle 110\rangle}$ | | | | $Si_{TC}$ |
| $SiC_{\langle 110\rangle}$ | $Si_{TC}$ | | | | $Si_{TC}$ |

Our results (GGA) are compared with other studies carried out using LDA [15] and LSDA [16–18]. If a defect is converted into another one during the relaxation, it is indicated instead of the formation energy. $H_C$ corresponds to a carbon atom in a hexagonal site and $W_C$ ($E_f = 6.3$ eV in [18]) to an intermediate defect between $CSi_{\langle 110\rangle}$ and $CC_{\langle 100\rangle}$, actually close to $CC^*_{\langle 100\rangle}$, the tilted $CC_{\langle 100\rangle}$ configuration.

For the carbon vacancy, the formation energy computed from our GGA calculations is 3.63 eV, slightly below the values determined with LDA. The local symmetry remains $T_d$, in contradiction with a previous study [17], where a Jahn–Teller distortion increased the vacancy stability. The neglect of spin polarization in our work is a possible explanation for this difference.

The formation energy for the silicon vacancy is 7.48 eV, 0.5–1 eV smaller than LDA values. Here, the system gains energy by shortening the distance between the first- and second-nearest neighbors of the vacancy. The distance between two carbon neighbours around the silicon vacancy is extended to 3.41 Å compared to the characteristic distance in bulk SiC 3.10 Å. The symmetry of the silicon vacancy is $T_d$.

### 3.2. Antisites

According to theoretical predictions, the carbon and silicon antisite are electrically, optically and magnetically inactive and therefore, not observable experimentally [19].

In our work and all other calculations, the carbon antisite appears to have the lowest formation energy among intrinsic point defects, with only 3.48 eV. This defect has a $T_d$ symmetry and the relaxation shorten the carbon–carbon

bond lengths around the carbon antisite to 1.68 Å. Previous LDA calculations pointed out that a complex $V_C$–$C_{Si}$ is more stable than the silicon vacancy by 1.1 eV [20] and 1.8 eV [21], due to the low formation energies of both carbon vacancy and antisites. In our work, we found that the silicon vacancy formation energy is 0.37 eV higher than the sum of the formation energies of the carbon vancancy and the carbon antisite, which is in favour of the stability of the $V_C$–$C_{Si}$ complex.

For the silicon antisite, our computed formation energy is 4.02 eV, close to LDA calculation. During relaxation, the bond lengths with silicon first-neighbors increase by 14%, compared to the Si–C bond lengths.

### 3.3. Carbon interstitials

As a whole, our calculated formation energies for carbon interstitials are similar than in LDA calculations. Relative stability is also unchanged, as dumbbell interstitials (threefold coordinated) are preferred over tetrahedral interstitials (fourfold coordinated). In addition, in our calculations, tetrahedral interstitials are not stable and relaxed to a $CC_{\langle 100\rangle}$. We found that this dumbbell in its tilted configuration is the most stable defect. This configuration has been shown to be slightly more stable than the well oriented interstitial for almost all charge states [22]. The angle between the dumbbell bond and the $\langle 1\,0\,0\rangle$ direction is 31°, i.e. very close to the results of Bockstedte et al. [22]. The $C_i$–C bond length is 1.35 Å, even shorter than a carbon–carbon double bond. The $C_i$ carbon interstitial forms bonds with two silicon atoms, a stronger one with a bond length of 1.73 Å and a weaker one with a bond length of 1.97 Å. In their calculations, Lento et al. found that the most stable carbon interstitial is an intermediate defect (noted $W_C$) between the $CC_{\langle 100\rangle}$ and the $CSi_{\langle 100\rangle}$ dumbbell interstitial [18], very similar to the tilted $CC^*_{\langle 100\rangle}$ dumbbell. Next stable configurations are CC dumbbells with other orientations, or a CSi dumbbell, with slightly higher formation energies.

### 3.4. Silicon interstitials

The most stable silicon interstitial is the configuration $Si_{TC}$ with the Si atom surrounded by four carbon atoms, in agreement with other LDA calculations. The formation energy is 7.04 eV, very close to the value in [15], but 1 eV higher than another study [18]. The bond length between the silicon interstitial and the surrounding carbon atoms is 1.84 Å, whereas the distance between the interstitial and the nearest silicon atoms is 2.40 Å. The next stable configurations are $SiSi_{\langle 110\rangle}$ and $SiSi_{\langle 100\rangle}$ dumbbells, in relatively good agreement with previous studies. For the $SiSi_{\langle 1\bar{1}0\rangle}$ case, the Si–Si bond length is rather short with 2.15 Å, the distance between each dumbbell atom and carbon nearest-neighbor being 1.78 Å. Other configurations are not stable and relaxed to $Si_{TC}$ or SiSi dumbbells. A possible explanation is the lattice distortion which cannot sufficiently stabilize these configurations, as Si–Si bonds are too compressed.

## 4. Frenkel pairs

In a previous paper [7], Frenkel pairs have been obtained from a first principles molecular dynamics determination of threshold displacement energies. Similar Frenkel pair configurations, with close interstitial–vacancy separations, have been obtained in another work [23]. Configuration analysis indicates that essentially CC or CSi dumbbells and $Si_{TC}$ interstitials are present in Frenkel pairs, in very good agreement with the stability of single point defects presented in the previous section. Five Frenkel pair configurations have been selected from previous calculations and then relaxed in a larger cell (216 atoms), in order to increase the level of accuracy. Moreover, the exchange-correlation functional used in this study is different (GGA instead of LDA).

The Frenkel pairs can be classified according to two categories: the first one involving a carbon interstitial and a carbon vacancy $C_i$–$V_C$ and the second one involving a silicon vacancy and a silicon vacancy $Si_i$–$V_{Si}$ For each type of Frenkel pairs the relaxed structure is described below. As a whole, compared to LDA results, the main structural effect is an increase of bond lengths, well known for GGA functionals. The formation energies and the energetic difference with their corresponding isolated defects in their neutral charge state have been also calculated (Table 2).

### 4.1. $C_i$–$V_C$ Frenkel pairs

Three Frenkel pairs combining a carbon vacancy and a carbon interstitial are described, one with a $CC^*_{\langle 100\rangle}$ dumbbell and two other with $CSi_{\langle 100\rangle}$ dumbbell. This is in agreement with our calculations of single point defects, showing that these interstitials are the most stable in cubic silicon carbide.

The first Frenkel pair configuration (A) is a $CC^*_{\langle 100\rangle}$ dumbbell interstitial separated from the vacancy $V_C$ by $\sim 0.85a_0$, as shown in the Fig. 1. It is associated with a displacement energy of 18 eV on the carbon sublattice and has a formation energy of 9.90 eV. The bond length between the carbon interstitial and the other carbon atoms was found to be 1.35 Å, which is about 10% smaller than diamond bond length. As for single carbon interstitial, this

Table 2
Threshold displacement energies (determined in [7]) and formation energies ($E_f$) in eV for Frenkel pairs

| Frenkel pair | TDE | $E_f$ |
|---|---|---|
| A: $V_C + CC_{\langle 100\rangle}$ | 18 | 9.90 |
| B: $V_C + CSi_{\langle 0\bar{1}0\rangle}$ | 14 | 6.73 |
| C: $V_C + CSi_{\langle 010\rangle}$ | 16 | 9.96 |
| D: $V_{Si} + Si_{TC}$ | 46 | 14.08 |
| E: $V_{Si} + Si_{TC}$ | 22 | 13.46 |

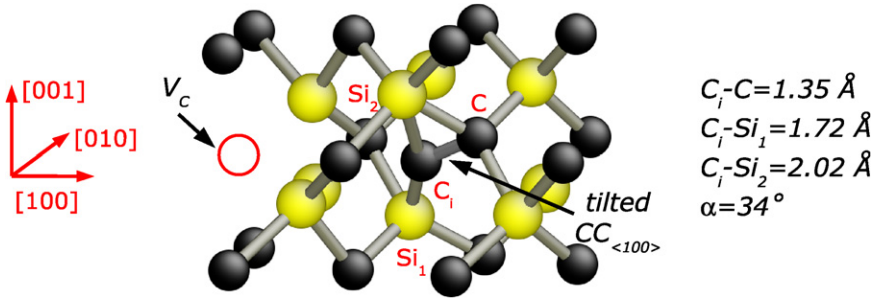


Fig. 1. Frenkel pair A: relaxed configuration for a $CC^{*}_{\langle 100\rangle}$ tilted dumbbell with a vacancy–interstitial separation of $\sim 0.85a_0$. Si (C) atoms are drawn as light (dark) grey spheres. Relevant interatomic distances and angles are specified.

dumbell configuration is not strictly oriented along the $\langle 100\rangle$ direction, but with a tilting angle of 34°. The interatomic distances between the carbon interstitial and the two nearest silicon atoms are $C_i$–$Si_1 = 1.72$ Å and $C_i$–$Si_2 = 2.02$ Å.

The second Frenkel pair configuration (B) is a $CSi_{\langle 100\rangle}$ dumbbell interstitial separated from the $V_C$ vacancy by $\sim 0.5a_0$, as shown in the Fig. 2. This configuration is very stable in spite of the short Frenkel pair separation. In fact the formation energy of this Frenkel pair is even smaller than the formation energy needed for a single $CSi_{\langle 100\rangle}$ dumbbell interstitial. A possible explanation is a weakening in the Frenkel pair of the $sp^2$ hybridization, energetically unfavorable for silicon. In fact, compared to the isolated interstitial, only the carbon atom of the dumbbell shows an $sp^2$ hybridization. Instead, due to the lattice distortion, the dumbbell silicon atom remains in a $sp^3$ hybridized state, with four strong bonds, one with the carbon interstitial ($C_i$–Si = 1.77 Å instead of $C_i$–Si = 1.71 Å in the isolated $CSi_{\langle 100\rangle}$), one with another carbon atom and two with silicon atoms (Si–Si distances shorter than in bulk silicon). With such a configuration, only one dangling bond remains around the carbon vacancy.

Another Frenkel pair involving a $CSi_{\langle 100\rangle}$ dumbbell interstitial is denoted C in the Fig. 3 and is obtained for a displacement energy of 16 eV. In this configuration, the vacancy–interstitial separation is about $0.95a_0$. Here, a distortion of the $CSi_{\langle 100\rangle}$ dumbbell also occurs due to the vicinity of the vacancy, but contrary to the B configuration, the silicon remains hybridized $sp^2$. As a consequence, the

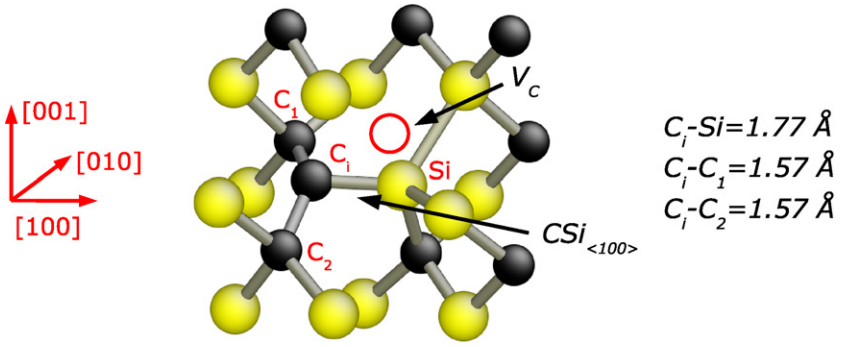


Fig. 2. Frenkel pair B: relaxed configuration for a $CSi_{\langle 100\rangle}$ dumbbell with a vacancy–interstitial separation of $\sim 0.50a_0$. See the caption of Fig. 1 for further details.

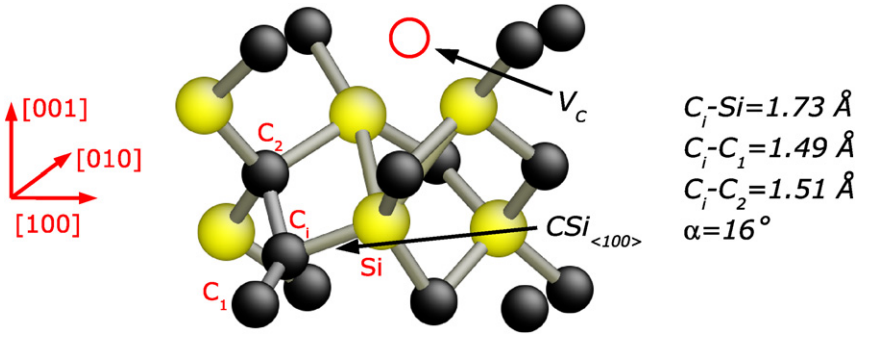


Fig. 3. Frenkel pair C: relaxed configuration for a $CSi_{\langle 100\rangle}$ dumbbell with a vacancy–interstitial separation of $\sim 0.95a_0$. See the caption of Fig. 1 for further details.

formation energy is much larger than in the B case. The distance $C_i$–Si becomes 1.73 Å and this bond is now tilted by 16° with respect to the ⟨1 0 0⟩ axis.

### 4.2. $Si_i$–$V_{Si}$ Frenkel pairs

Two Frenkel pairs combining a silicon vacancy and a silicon interstitial are described, both with a $Si_{TC}$, i.e. a tetrahedral interstitial surrounded by four carbon atoms. As detailed in the previous section this interstitial have been determined as the most stable silicon interstitial in all calculations and 1.07 eV below the $SiSi_{\langle 110\rangle}$ dumbbell interstitial in our calculations.

In the first Frenkel pair (noted D), shown on Fig. 4, the distance between the $Si_{TC}$ interstitial and the vacancy is $\sim 1.5a_0$. In this case, the vacancy and the $Si_{TC}$ interstitial are in line along the ⟨1 0 0⟩ direction. The bond length between the silicon interstitial and the surrounding carbon atoms is 1.84 Å, whereas bond lengths between the interstitial and the nearest silicons are 2.41 Å.

The separation between the $Si_{TC}$ interstitial and the vacancy is slightly larger for the other Frenkel pair (E), with $\sim 0.9a_0$ (Fig. 5). In this configuration, vacancy and interstitial are located along the ⟨1 1 1⟩ direction. The bond lengths between the silicon interstitial and nearest carbon atoms, as well as between the interstitial and the nearest silicon atoms, are similar than in the configuration D, with values of 1.83–1.84 Å and 2.41–2.42 Å, respectively. Despite a larger vacancy–interstitial separation in E than in D, it appears that both configurations show quite similar structures.

## 5. Discussion

Due to the strong covalent characters of bonding in silicon carbide, Frenkel pairs are stable even for very small vacancy–interstitial separations. Then, a large interaction between the vacancy and the interstitial is expected. Since one interstitial tends to introduce a local deformation of the lattice and a vacancy provides space for accommodating this distortion, it is expected that this interaction is attractive. In this work, we focus on Frenkel pairs generated by displacement energies simulations and our configurations set is too small to make a complete investigation of the vacancy–interstitial interaction. However, meaningful insights can be obtained by comparing similar configurations with different vacancy–interstitial separations, such as B and C, or D and E. In the latter case, the separations are $\sim 1.5a_0$ (D) and $\sim 0.9a_0$ (E). As expected, the formation energy for D is lower than for E, suggesting an attractive vacancy–interstitial interaction. In the B–C case, the separations are $\sim 0.5a_0$ (B) and $0.95a_0$ (C). Again, the formation energy for the shortest separation is the lowest.

Another way to get insights about the interaction between interstitial and vacancy is to study of the Frenkel pairs stability with respect to isolated single defects. Then, we have compared the formation energies in both cases, by computing the energy difference $\Delta E = E_f^{FP} - (E_f^V + E_f^I)$. $E_f^I$

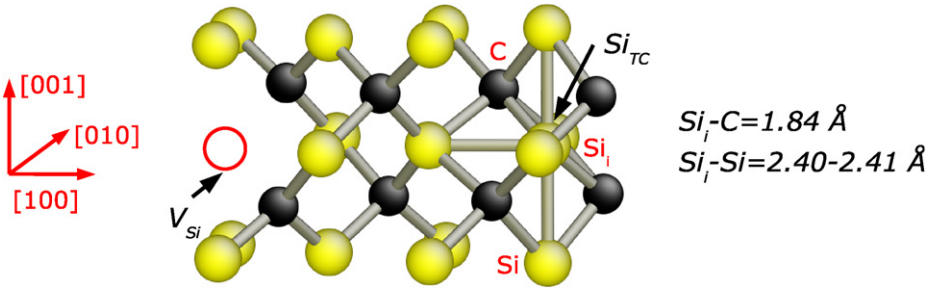


Fig. 4. Frenkel pair D: relaxed configuration for a $Si_{TC}$ tetrahedral interstitial with a vacancy along the [1 0 0] direction. See the caption of Fig. 1 for further details.

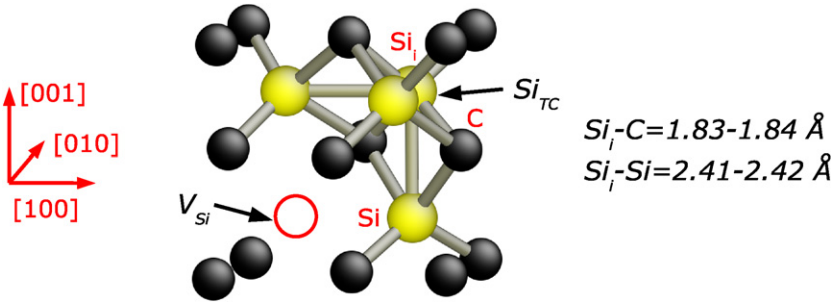


Fig. 5. Frenkel pair E: relaxed configuration for a $Si_{TC}$ tetrahedral interstitial with a vacancy along the [1 1 1] direction. See the caption of Fig. 1 for further details.

is the formation energy of the most stable interstitials, i.e. $Si_{TC}$ for silicon and $CC^{*}_{\langle 100\rangle}$ for carbon. Regarding carbon interstitials, there are no significant differences for A ($\Delta E = -0.03$ eV) and C ($\Delta E = +0.03$ eV), whereas the Frenkel pairs B is much more stable than isolated defects ($\Delta E = -3.20$ eV). For silicon interstitials, the Frenkel pairs are more stable, with significant energy differences ($\Delta E = -0.44$ eV for D and $\Delta E = -1.06$ eV for $E$). Overall, our results suggest that Frenkel pairs with short interstitial–vacancy separations tend to be more stable than isolated defects, confirming the attractive interstitial–vacancy interaction. This behaviour have been also observed in silicon by Mazzarolo et al. [24].

## 6. Conclusion

Intrinsic point defects and Frenkel pairs obtained from displacement energies determination have been relaxed using first principles DFT-GGA calculations. These defects have been characterized, both structurally and energetically. We have found that the most stable carbon interstitial is a tilted CC dumbbell, whereas a Si interstitial in tetrahedral site $Si_{TC}$ is favored. Although we used GGA in our calculations, our results are in agreement with previous LDA studies (in neutral state and stoichiometric conditions). We have shown that Frenkel pairs are more stable than isolated single defects, especially for silicon interstitials, indicating that the interaction between the vacancy and the interstitial is attractive, as expected.

## Acknowledgement

This work was funded by the joint research program "ISMIR" between CEA and CNRS.

## References

[1] H. Hensel, H.M. Urbassek, Nucl. Instr. and Meth. B 142 (1998) 287.
[2] W. Windl, T.J. Lenosky, J.D. Kress, A.F. Voter, Nucl. Instr. and Meth. B 141 (1998) 61.
[3] R. Devanathan, W.J. Weber, J. Nucl. Mater. 278 (2000) 258.
[4] L. Malerba, J.M. Perlado, A. Sánchez-Rubio, I. Pastor, L. Colombo, T. Diaz de la Rubia, J. Nucl. Mater. 283–287 (2000) 794.
[5] R. Devanathan, W.J. Weber, F. Gao, J. Appl. Phys. 90 (2001) 2303.
[6] L. Malerba, J.M. Perladoa, Phys. Rev. B 65 (2003) 045202.
[7] G. Lucas, L. Pizzagalli, Phys. Rev. B 72 (2005) 161202.
[8] P. Hohenberg, W. Kohn, Phys. Rev. 136 (1964) B864.
[9] W. Kohn, L.J. Sham, Phys. Rev. 140 (1965) A1133.
[10] S. Baroni, A. Dal Corso, S. de Gironcoli, P. Giannozzi, C. Cavazzoni, G. Ballabio, S. Scandolo, G. Chiarotti, P. Focher, A. Pasquarelloa, K. Laasonen, A. Trave, R. Car, N. Marzari, A. Kokalj, http://www.pwscf.org/.
[11] J.P. Perdew, K. Burke, M. Ernzerhof, Phys. Rev. Lett. 77 (1996) 3865.
[12] D. Vanderbilt, Phys. Rev. B 41 (1990) 7892.
[13] C.G. Broyden, J. Inst. Math. Appl. 6 (1970) 70.
[14] S.B. Zhang, J.E. Northrup, Phys. Rev. Lett. 67 (1991) 2339.
[15] M. Salvador, J.M. Perlado, A. Mattoni, F. Bernardini, L. Colombo, J. Nucl. Mater. 329–333 (2004) 1219.
[16] A. Gali, P. Dek, E. Rauls, N.T. Son, I.G. Ivanov, F.H.C. Carlsson, E. Janzn, W.J. Choyke, Phys. Rev. B 67 (2003) 155203.
[17] A. Zywietz, J. Furthmüller, F. Bechstedt, S.T. Picraux, Phys. Rev. B 59 (1999) 15166.
[18] J.M. Lento, L. Torpo, T.E.M. Staab, R.M. Nieminen, J. Phys.: Condens. Matter 16 (2004) 1053.
[19] L. Torpo, M. Marlo, T.M.E. Staab, R.M. Nieminen, J. Phys.: Condens. Matter 13 (2001) 6203.
[20] M. Bockstedte, A. Mattausch, O. Pankratov, Phys. Rev. B 69 (2004) 235202.
[21] E. Rauls, Annealing mechanism of defects in silicon carbide, Ph.D. thesis, Universität Paderborn, 2003.
[22] M. Bockstedte, A. Mattausch, O. Pankratov, Phys. Rev. B 68 (2003) 205201.
[23] F. Gao, W.J. Weber, J. Appl. Phys. 94 (2003) 4348.
[24] M. Mazzarolo, L. Colombo, G. Lulli, E. Albertazzi, Phys. Rev. B 63 (2001) 195207.